Gamma Rays from Short-Lived Fission-Fragment Isomers*

R. E. SUND AND R. B. WALTON
General Atomic Division of General Dynamics Corporation, John Jay Hopkins Laboratory for Pure and Applied Science, San Diego, California
(Received 26 January 1966)

Measurements of the energy spectra of isomeric gamma rays from the neutron fission of U^{235} and Pu^{239} at a number of time intervals between 50 and 600 μsec showed six prominent gamma rays for both cases of fission. The intensities and half-lives for these gamma rays indicate that there are three fission-fragment isomers, each giving rise to a pair of gamma rays in cascade. The energies of the cascade gamma rays and the half-life for each isomer are: 1260, 450 keV (80 μsec), 850, 250 keV (54 μsec), and 990, 710 keV (32 μsec). Absolute gamma-ray intensities were obtained by measuring the integral number of gamma rays above a fixed bias energy as a function of time and normalizing these data at 10 msec to the absolute intensities derived from the theoretical work by Griffin and the data of Fisher and Engle. The intensities of delayed gamma rays from photofission of U^{235}, Pu^{239}, and U^{238} were also measured at early times, starting at 2 μsec after fission. An intense short-lived component with an apparent half-life of a few μsec was observed for all three cases of photofission.

I. INTRODUCTION

EVIDENCE for short-lived isomers formed either directly in the fission process or following emission of prompt neutrons and gamma rays by the initial fission fragments was first obtained by Maienschein, Peelle, Zobel, and Love[1] from measurements of gamma rays emitted between 10 nsec and 1 μsec after the thermal-neutron fission of U^{235}. Recently, Johansson[2] observed that isomers with half-lives ranging between 15 nsec and 100 nsec are formed by the spontaneous fission of Cf^{252}. In a previous measurement[3] of delayed gamma rays emitted between 100 μsec and 7 sec after the photofission of U^{238}, U^{235}, and Th^{232}, we found that isomers with half-lives of the order of 70 μsec are produced copiously in fission and are the dominant source of delayed gamma rays for times less than 500 μsec after fission. Beyond 1 msec, the observed rate of gamma-ray emission decreased little in the interval up to 0.1 sec. Such a "plateau region" was expected for gamma rays arising from beta decay of fission fragments to excited states of daughter nuclei since the half-life for beta decay of fragments generally exceeds 0.1 sec.

This paper presents the results of measurements of delayed gamma rays emitted from the neutron fission of Pu^{239} and U^{235} at times ranging from ~50 μsec to the plateau region. The energies and relative intensities of the gamma rays and the half-lives of the corresponding isomeric states were obtained from gamma-ray pulse-height distributions measured with a NaI detector in several time intervals between 50 μsec and 600 μsec. The intensities of the isomeric gamma rays were fixed relative to the gamma-ray intensity in the plateau region by measuring the intensity of gamma rays having energies greater than a selected bias energy as a function of time between ~100 μsec and 30 msec. The intensity-versus-time data were normalized to the absolute intensities in the plateau region which were derived from the theoretical work of Griffin[4] and the experimental data of Fisher and Engle for times greater than 0.2 sec after fission.[5] All of these data were then combined to obtain a complete description of delayed gamma rays from $Pu^{239}(n,F)$ and $U^{235}(n,F)$ in the interval from 50 μsec to the plateau region. The number of isomers giving rise to the prominent gamma rays observed in this time interval and their absolute fission yields were obtained from the delayed gamma-ray data.

The present investigation also included a search for fission-fragment isomers with half lives of the order of several μsec. This search consisted of measuring the intensity of delayed gamma rays from the photofission of Pu^{239}, U^{238}, and U^{235} as a function of time over the interval from 2 μsec to 200 μsec. The measurements for Pu^{239} were extended to the plateau region since no photofission data had previously been taken for this isotope.

II. DELAYED GAMMA RAYS FROM NEUTRON FISSION OF U^{235} AND Pu^{239}

A. Experimental Setup

A schematic drawing of the experimental configuration used for these measurements is provided in Fig. 1. Neutrons produced by bombarding a target with a pulse of 28-MeV electrons from the General Atomic linear accelerator caused a burst of fissions in a U^{235} or Pu^{239} sample located inside a shielded cavity. Instantaneous electron-beam currents up to 400 mA were avaliable at the target position, and the duration of the

* This work was supported by the U. S. Air Force Weapons Laboratory.
[1] F. C. Maienschein, R. W. Peelle, W. Zobel, and T. A. Love, in *Second United Nations Conference on the Peaceful Uses of Atomic Energy, Geneva, 1958* (United Nations, Geneva, 1958), Vol. 15, p. 366.
[2] S. A. E. Johansson, Nucl. Phys. 64, 147 (1965).
[3] R. B. Walton, R. E. Sund, E. Haddad, J. C. Young, and C. W. Cook, Phys. Rev. 134, B824 (1964).
[4] J. Griffin, Phys. Rev. 134, B817 (1964).
[5] P. C. Fisher and L. B. Engle, Phys. Rev. 134, B796 (1964).

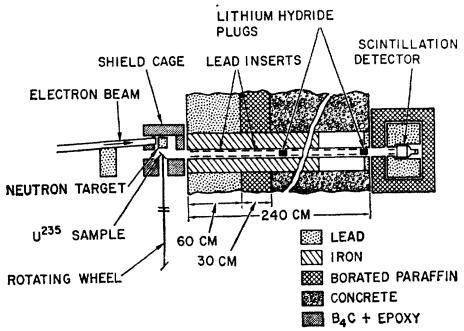

FIG. 1. Schematic drawing of the configuration used for studies of delayed gamma rays from neutron fission.

electron beam was variable from 10 nsec to 5 μsec. During a data recording period the neutron source strength was monitored by measuring the charge deposited on the target by the beam with a current integrator. Delayed gamma rays from the sample were measured with a scintillation detector which viewed the sample through a 4.5-cm diameter collimating hole in a 2.4-m thick shield wall. LiH plugs having a total thickness of 6 g/cm^2 were placed in the collimator to prevent neutrons from traveling through the collimator to the detector.

Ten identical fission samples were mounted on a rotating wheel which triggered the accelerator each time a new sample arrived inside the shielded cavity. The highest beam repetition rate that could be utilized without generating excessive background activity in the samples was one pulse per second. Each of the U^{235} samples consisted of eight U^{235} foils, each 0.013 cm thick, interlaced with seven 0.32-cm sheets of pure polyethylene. The polyethylene moderated the fast neutrons from the target, thereby boosting the fission yield to a level adequate for measurements extending to the plateau region. Each Pu^{239} sample consisted of four 0.025-cm foils interlaced with 0.64-cm sheets of polyethylene. Each Pu foil was clad with 0.0076-cm nickel foil and sealed between two 0.038-cm layers of plastic.

Details of the arrangement of the sample, neutron source, and the shielded cavity are shown in Fig. 2. The neutron source consisted of a piece of U^{238} embedded in a block of lead, which attenuated the "beam flash" of bremsstrahlung x rays. The walls of the cavity, which were made of B_4C and epoxy, served as a neutron shield for the fission samples located outside the cavity and also prevented neutrons from escaping into the room and creating a time-dependent background. In addition, the inner walls of the cavity were lined with cadmium and indium to further diminish the number of low-energy neutrons reflected from the walls back into the fission sample at times of interest for delayed gamma-ray measurements.

Two different detection systems were used to gather the data on delayed gamma rays from neutron fission. The first, which was used for measurements of gamma-ray energy spectra in the isomeric region, was a 7.6-cm diam by 7.6-cm long NaI crystal mounted on a standard 10-stage photomultiplier tube. Signals from the photomultiplier passed through a cathode follower to a Hammer A-8 amplifier, the output of which passed through a time gate to a TMC pulse-height analyzer. This system permitted the measurement of pulse-height distributions of the gamma rays emitted within a preselected time interval after the beam pulse.

The second detection system, consisting of a 5.1-cm diam by 2.5-cm thick plastic (Pilot B) scintillator mounted on a 10-stage photomultiplier tube, was used to measure the intensity of delayed gamma rays as a function of time from about 100 μsec to 25 msec after fission. The signals from this detector were amplified by a Hammer A-8 amplifier, and the pulses from the integral bias discriminator of the amplifier were fed into a 1024-channel TMC time analyzer. The gamma-ray efficiency of this detector for an integral bias of 510 keV had been measured previously.[3] The TMC time analyzer was triggered ahead of the accelerator beam pulse by about 100 time channels in order to measure the long-lived activity of the sample and its surroundings immediately preceding the burst of fissions. The intensity-versus-time data obtained with this system, corrected for the detector efficiency and the attenuation of the gamma rays by the sample and the LiH plugs, were proportional to the yield of photons (with energies $E_\gamma > 510$ keV) per fission sec.

The most difficult aspect of the measurements performed with the neutron-fission setup was the determination of the time-dependent background produced by the interaction of neutrons with the fission sample, the cavity, and the collimation system. This background may be understood qualitatively from the following arguments about the sequence of events following a beam pulse. A large portion of the fast neutrons from the target strike the sample and are scattered by the fission foils and polyethylene while the remainder are thermalized in the sample where they either get absorbed or leak out with a characteristic die-away time of a few μsec. The desired burst of fissions, which is generated by a portion of the neutrons which are

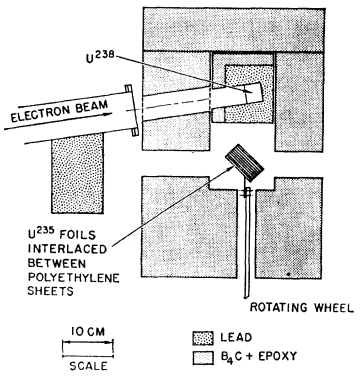

FIG. 2. Details of the sample and source configuration for measurements of delayed gamma rays from neutron fission.

absorbed in the sample, also gives rise to additional fast neutrons which may contribute to the time-dependent background. Although the fission burst width is effectively only a few μsec, there are a sufficient number of slow neutrons surviving in the sample for times up to $\sim$50 μsec to cause a background which is appreciable relative to the delayed gamma-ray signal. Most of the fast neutrons which enter the 2.4-m-thick shield wall shown in Fig. 1 are thermalized and subsequently give rise to a background with a characteristic lifetime of the order of 200 μsec.

The time-dependent backgrounds generated by neutrons were determined from measurements performed with background subtraction samples which simulated as closely as possible all properties of the fission samples except, of course, the fission-delayed gamma rays. The background samples contained the same amount of polyethylene as the fission samples and, in the case of the sample simulating the Pu sample, the same amount of nickel as contained in the cladding for the Pu foils. In addition, the background samples contained cadmium and iron foils to simulate the absorption and scattering of neutrons by the fission foils. The thickness of the cadmium foils was chosen to give the same macroscopic absorption cross section as the fission foils in order to match the thermal-neutron dieaway time of the fission sample. Since the gamma-ray yield from neutron capture by cadmium is different from that from neutron absorption by U^{235} and Pu^{239}, the signals from the background samples were not expected to match the actual background produced by absorption of thermal neutrons by the fission samples. However, this did not constitute a problem for delayed gamma-ray data recorded after the thermal neutrons had disappeared from the vicinity of the sample, i.e., at times greater than 50 μsec after the beam pulse.

In an attempt to simulate the scattering and production (by fission) of fast neutrons by the fission foils, a total thickness of 0.25-cm iron was included in the background samples; however, because of the neutron multiplication resulting from fissions, an exact simulation was not possible with this method. To estimate the consequent mismatch of the background samples to the fission samples, the relative number of fast neutrons emanating from each of the samples and passing through the collimator (Fig. 1) was measured. The fast-neutron detector consisted of a BF_3 detector embedded in paraffin, the outside of which was covered with a thick layer of cadmium. The LiH plugs were removed from the collimation system to permit free passage of neutrons from the samples to the detector. The number of fast neutrons from the fission sample was found to exceed that from its corresponding background subtraction sample by 30%. These measurements were then repeated with the BF_3 detector surrounded only by cadmium to compare the relative numbers of epicadmium neutrons emanating from the samples. Neutron yields from the background samples were approximately 5% larger than those from the fission samples. In addition, the gamma-ray intensity as a function of time was measured with a plastic scintillation detector for several different thicknesses of iron and cadmium. From these data and the neutron measurements it was estimated that the backgrounds determined using the background subtraction samples may be too low by a maximum of 30%. Therefore, the procedure adopted for the measurements was to scale the backgrounds determined with the background samples by a factor of 1.15($\pm$15%) before proceeding with the data reduction.

B. Gamma-Ray Energy-Spectrum Measurements

Pulse-height spectra were taken in five different time regions from 50 to 600 μsec after $Pu^{239}(n,F)$ and in three different time regions from 100 to 600 μsec after $U^{235}(n,F)$. Figure 3 shows a typical pulse-height spectrum, which was recorded between 50 and 100 μsec after $Pu^{239}(n,F)$. These data are not corrected for the background. For comparison, the spectrum from the background sample taken in the same time interval is also shown in this figure. The energies of the fission gamma rays were determined from a simultaneous pulse-height measurement of the gamma rays from the fission sample and the gamma rays from a Na^{22} source which was placed near the detector. This method circumvented possible errors in the energy calibration due to electronic gain shifts caused by the beam flash. The energy calibration showed that the six strong gamma rays from the Pu sample had energies of 250, 450, 710, 850, 990, and 1260 keV.

The pulse-height spectra taken in various time intervals after $Pu^{239}(n,F)$ are shown in Fig. 4. These gamma-ray spectra were normalized to the product of the integrated beam current and the width of the time interval for the run. For clarity, smooth curves instead of actual data points were used to display the spectral information. The total number of counts in the 450-keV photopeak in the original data varied between a minimum of 162 for the 400- to 600-μsec spectrum to a maximum of 450 for the 200- to 300-μsec spectrum. The spectra taken with the background sample were not subtracted from the data shown in Fig. 4. For energies above 400 keV the background spectra for all of the time intervals were roughly the same intensity relative to the uncorrected Pu data as shown in Fig. 3. For energies below 400 keV the spectrum from the background sample relative to that from the Pu sample increased with the time after fission. In the interval from 400 to 600 μsec the spectrum from the background sample increased monotonically for decreasing energies below 400 keV, being about equal to that for the Pu sample at 370 keV and a factor of 2 larger at 175 keV. These data indicate that the background sample was somewhat mismatched, particularly at low energies.

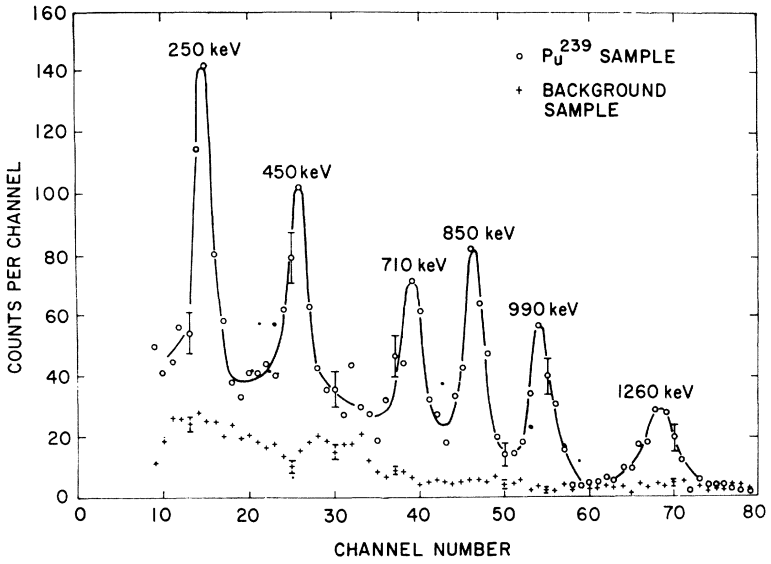

FIG. 3. Pulse-height spectrum of gamma rays from the Pu^{239} sample between 50 and 100 μsec after neutron fission. For comparison, the spectrum from the background sample taken in the same time interval and normalized to the same beam monitor reading as that for the Pu data is also shown.

Except for a small bump which occurred in the region of 525 keV, no photopeaks were apparent in any of the spectra from the background samples. This bump was attributed to gamma rays from the decay of the 132-μsec Pb^{206} isomer formed in the lead collimation system by inelastic neutron scattering. A measurement of the energy spectrum and decay of the gamma rays from a lead sample showed that this isomer is produced copiously by inelastic neutron scattering.

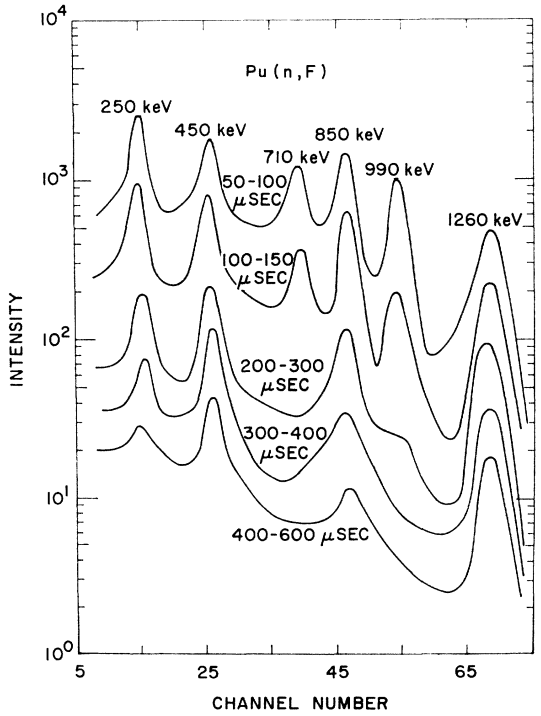

FIG. 4. Gamma-ray pulse-height spectra in various time intervals after $Pu^{239}(n,F)$.

Figure 5 shows the pulse height distribution of gamma rays emitted from the lead sample in the interval from 200 to 400 μsec after the beam pulse. Measurements taken with W instead of Pb proved that the photopeaks in this spectrum were from lead. The present results for the gamma-ray energies and the half-life are in good agreement with the results obtained by others using different reactions to produce this isomer.[6] The weak 343-keV gamma ray was obscured by the Compton tails of the higher energy gamma rays and by the background, which was larger at the lower energies.

Figure 6 shows half-life plots for the six gamma rays observed in the Pu spectra. The relative decay rate for a particular gamma ray was determined by summing the counts under its photopeak in the spectra for the various time intervals. Small corrections were made to

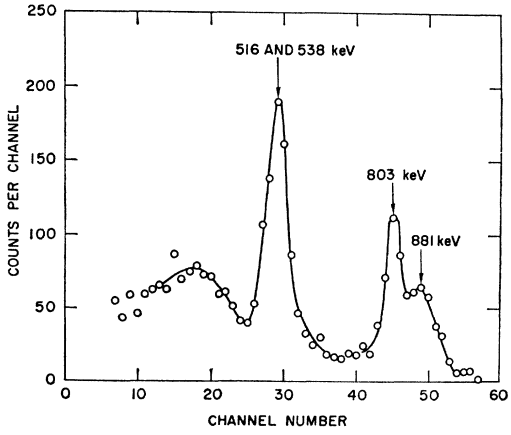

FIG. 5. Gamma-ray pulse-height spectrum between 200 and 400 μsec after the excitation Pb^{206} by inelastic neutron scattering.

[6] D. E. Alburger and M. H. L. Pryce, Phys. Rev. **95**, 1482 (1954); S. H. Vegors, Jr., and P. Axel, *ibid.* **101**, 1967 (1956).

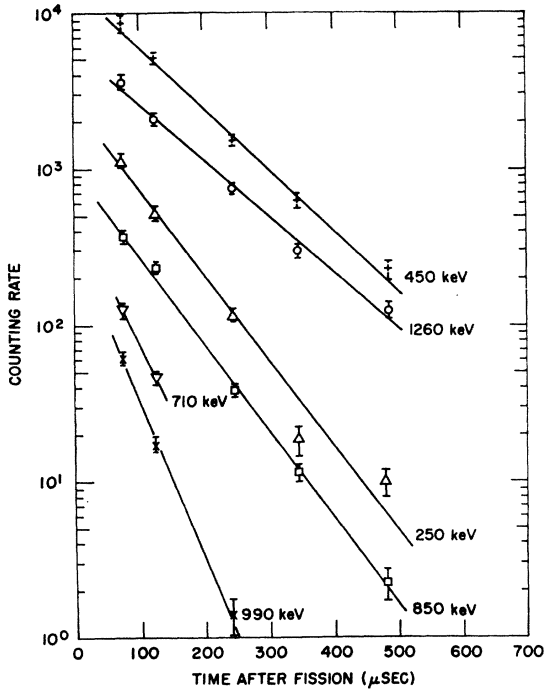

FIG. 6. Half-life plots for the gamma rays observed following $Pu^{239}(n,F)$.

the data for the analyzer dead time. The relative intensity of each of the gamma rays shown in the half-life plots was normalized arbitrarily for convenience of plotting, and corrections were made to the times at which the data points were plotted to account for the half-life of the transition and the width of the time interval. Least-squares fits to the data (except for the 710-keV gamma ray) were performed to determine the half-lives for the transitions and the relative intensities of the photopeaks at 100 μsec after fission. These intensities were then corrected for the photopeak-to-total ratios, the crystal efficiency, and the attenuation of the gamma rays in the Pu sample and in the LiH plugs. The resulting relative intensities were normalized to absolute yields by summing the intensities of the 710-, 850-, 990-, and 1260-keV gamma rays and equating this sum to the absolute intensity of isomeric gamma rays with energies greater than 510 keV obtained from the intensity-versus-time measurements (Sec. IIC). This normalization was carried out at 100 μsec because the uncertainty in the evaluation of the background for the intensity-versus-time measurements was small at this time. The results for the half-lives and the absolute intensities at 100 μsec are given in Table I. The errors given in this table are due only to the uncertainties in the pulse-height distribution data.

Similar spectra taken from 100 to 200, 200 to 400, and 400 to 600 μsec after $U^{235}(n,F)$ showed the same six gamma rays. Absolute intensities obtained from these are also given in Table I.

TABLE I. Energies, half-lives, and absolute intensities of isomeric gamma rays at 100 μsec after neutron fission of Pu^{239} and U^{235}.

Energy (keV)	Half-life (μsec)	Absolute intensity at 100 μsec after $Pu^{239}(n,F)$ (photons per fission-sec)	Absolute intensity at 100 μsec after $U^{235}(n,F)$ (photons per fission-sec)
250	55±4	28.4±3.3	33.1±3.4
450	77±4	17.3±1.5	10.0±2.5
710	35±6	15.0±1.5	8.6±2.2
850	53±3	25.8±2.0	30.3±2.2
990	30±3	13.2±1.3	8.9±2.5
1260	84±4	16.0±1.1	13.1±1.9

C. Intensity-Versus-Time Measurements

Figure 7 shows the intensity of delayed gamma rays as a function of time after $U^{235}(n,F)$, as measured with the plastic scintillator and an integral detector bias of 510 keV. The data shown in the figure have been corrected for long-lived activities induced in the fission samples and collimation system by previous beam pulses but have not been corrected for the time-dependent neutron background. For comparison, the latter background, which was determined from measurements made with the background subtraction sample, is also shown in this figure. The background data were scaled up by the factor 1.15, as discussed above. The error bars shown in the figure denote

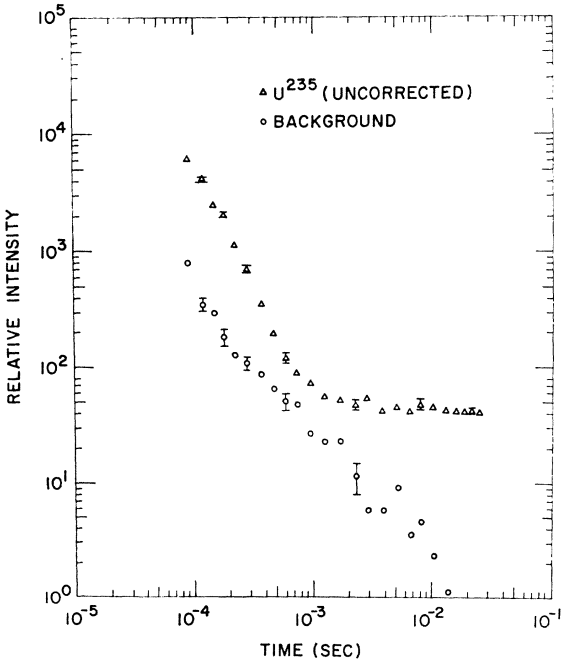

FIG. 7. Relative intensity of gamma rays versus time after the neutron fission of U^{235} for a discriminator bias setting of 510 keV (uncorrected for background). Also shown is a plot of the background which was determined with the background subtraction sample.

statistical uncertainties only. Similar data were obtained for $Pu^{239}(n,F)$.

After the backgrounds were subtracted from the U^{235} and Pu^{239} data, corrections were made for the energy dependence of the detector efficiency and the attenuation by the sample and LiH plugs using the procedure described in Ref. 3. The isomeric component of the data was separated from the plateau level, multiplied by the correction factor $I_{\text{Plateau}}/I_{\text{Isomer}}$, and then recombined with the plateau level of intensity. The quantities I_p and I_I were computed from the same general expression:

$$I=\int_{E_b}^{\infty} N_\gamma(E)\mathcal{A}(E)\epsilon_b(E)dE \Big/ \int_{E_b}^{\infty} N_\gamma(E)dE,$$

where $N_\gamma(E)$=energy spectrum of gamma rays, $\mathcal{A}(E)$=attenuation and $\epsilon_b(E)$=detector efficiency with bias E_b. The energy spectra for $Pu^{239}(n,F)$ and $U^{235}(n,F)$ which were measured by Fisher and Engle[5] at 0.35 sec after fission were used to calculate I_p. It was assumed that the shape of this spectrum did not change throughout the plateau region. I_I was calculated as a function of time using the *relative* gamma-ray intensities and the half-lives obtained from the measurements with the NaI detector (Sec. IIB). The resulting correction factors for Pu and U^{235} differed by only a few percent and varied monotonically between approximately 1.1 at 50 μsec at 0.85 at 600 μsec.

The corrected integral-bias data were then normalized in the plateau region near 10 msec to the absolute yields of photons with $E_\gamma>510$ keV which were derived from the plateau rates of gamma-ray energy emission given by Griffin[4] and the gamma-ray energy spectra obtained by Fisher and Engle[5] at 0.35 sec after fission. Figure 8 shows these normalized data. The statistical uncertainties, which are denoted by the error bars in the figure, were usually less than $\pm 15\%$. A systematic error was caused by the uncertainty of $\pm 15\%$ estimated for the factor 1.15 used to scale the data obtained with the background subtraction samples. The resulting systematic error as a function of time for both the U^{235} and Pu^{239} data is: $\pm 2\%$ at 100 μsec, $\pm 8\%$ at 600 μsec, $\pm 15\%$ at 700 μsec, $\pm 8\%$ at 1000 μsec, and 0% for times greater than 5000 μsec. An uncertainty of $\pm 10\%$ resulted from the corrections for detector efficiency and gamma-ray attenuation, and an uncertainty of $\pm 15\%$ resulted from the uncertainty in the $U^{235}(n,F)$ delayed gamma-ray data which Griffin used to fix the parameters in his theory.[4] Furthermore, an error may be present in the absolute intensities because the validity of some of the β-decay data which Griffin[4] used to establish the parameters in his theory has recently been questioned.[7] However, it is felt that

[7] J. J. Griffin, private communication, with reference to paper reported by H. J. Specht and H. Seyfarth at the International Conference on Nuclear Fission Physics, Salzburg, Austria, 1965.

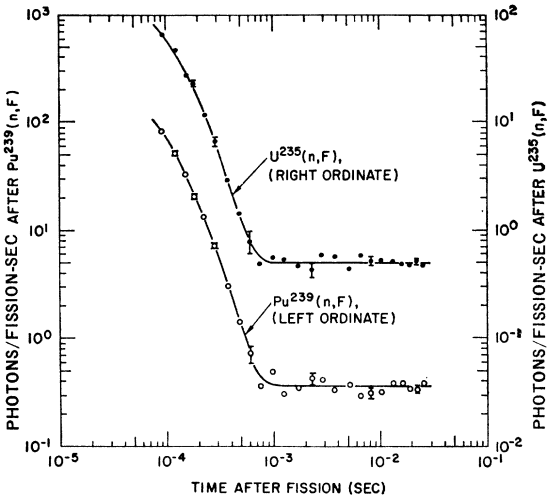

FIG. 8. Absolute intensities of gamma rays (photons/fission sec) with $E_\gamma>510$ keV as a function of time after $U^{235}(n,F)$ and $Pu^{239}(n,F)$.

the error reflected in Griffin's gamma-ray intensities in the plateau region is probably less than 15% since his calculations adequately fit the absolute gamma-ray intensity data of Fisher and Engle[5] at times greater than 0.35 sec after fission, and the shapes of Griffin's beta decay curves for times less than 0.35 sec agree within about 15% with the recent beta emission data of Specht and Seyfarth.[7] The rms of all these uncertainties in the absolute delayed gamma-ray data presented in Fig. 8 is $\sim 30\%$.

The absolute intensity of isomeric gamma rays with $E_\gamma>510$ keV versus time was also calculated from the half-lives and the absolute intensities given in Table I. The results agreed within experimental errors with the data measured with the plastic scintillator over the entire isomeric time region, which indicates that the methods used to reduce the data were consistent.

Absolute intensities of all gamma rays with energies greater than 140 keV, which were derived from the 510-keV bias data, the data in Table I, and the plateau values obtained from the work of Griffin[4] and Fisher and Engle,[5] are shown in Fig. 9. The intensities were extrapolated from 50 μsec to 10 μsec assuming that only the six gamma rays listed in Table I are emitted during this interval. Additional gamma rays with shorter half-lives than the observed transitions would make the intensities larger in the extrapolated region.

Figure 10 shows the absolute gamma-ray energy emission rates (MeV/fission-sec) which were derived from the data. The average energy per photon for the isomeric gammas from both $Pu^{239}(n,F)$ and $U^{235}(n,F)$ increases from about 0.7 MeV/photon at $t=60$ μsec to ~ 0.8 MeV/photon at $t=600$ μsec. In comparison, the average energy per photon at 0.35 sec is 0.87 MeV/photon for $Pu^{239}(n,F)$ and 0.92 for $U^{235}(n,F)$.[5]

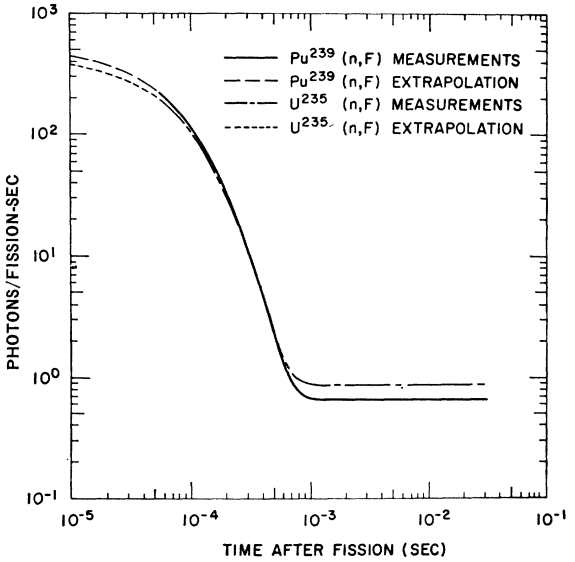

FIG. 9. Absolute intensities of gamma rays (photons/fission sec) with $E_\gamma > 140$ keV as a function of time after $U^{235}(n,F)$ and $Pu^{239}(n,F)$.

The absolute gamma-ray intensities and energy emission rates as a function of time are also given in Table II.

TABLE II. Absolute gamma-ray intensities and energy emission rates as a function of time after neutron fission for $E_\gamma > 140$ keV. The values for times less than 60 μsec were extrapolated assuming that only the six gamma rays listed in Table I are emitted.

Time (sec)	Absolute intensity (photons/fission sec) U^{235}	Pu^{239}	Absolute energy emission rate (MeV/fission sec) U^{235}	Pu^{239}
0	436	515	301	379
2×10^{-5}	323	375	221	273
4×10^{-5}	241	274	164	198
6×10^{-5}	184	204	123	149
8×10^{-5}	138	152	92	111
1×10^{-4}	104	116	70	83
1.5×10^{-4}	54	57	37	41
2×10^{-4}	30	32	21	23
3×10^{-4}	10.9	11.3	7.4	8.5
4×10^{-4}	4.3	4.6	3.3	3.7
5×10^{-4}	2.2	2.2	1.78	1.77
6×10^{-4}	1.41	1.28	1.18	1.05
7×10^{-4}	1.08	0.90	0.95	0.76
8×10^{-4}	0.95	0.74	0.85	0.64
1×10^{-3}	0.87	0.66	0.79	0.57
1.2×10^{-3}	0.85	0.64	0.78	0.56
2.5×10^{-2}	0.85	0.64	0.78	0.56

III. DELAYED GAMMA RAYS FROM PHOTOFISSION

A. Experimental Details

A pulsed beam of x rays for causing photofission was produced by bombarding a tungsten sample with 20-MeV electrons from the linear accelerator. The bremsstrahlung x rays were collimated by a hole in a 2.4-meter thick shield wall, beyond which were located a beam monitor, fission samples, and the gamma-ray detector. The collimation system transmitted an x-ray beam which was uniform within a well defined spot having a diameter of 5.1 cm at the sample position. The beam was monitored with a plastic scintillator mounted on an ITT photodiode tube, the current from which was proportional to the intensity of x rays transversing the scintillator.

Details of the geometry of the beam, sample, and detector are shown schematically in Fig. 11. The detector, which was positioned well out of the primary beam, consisted of a liquid organic scintillator (Nuclear Enterprise 211) contained in a glass cylinder 5 cm in diameter and 2.5 cm thick. A thin disk of aluminum was used to shield the detector from beta rays. A fission sample consisted of four identical units spaced 1.27 cm apart to reduce the attenuation of the delayed gamma rays by the sample. The dimensions of a single unit of the samples were

U^{235}, 5.1 cm by 3.5 cm (rectangular) by 0.842 g/cm^2 thick,
Pu^{239}, 5.1 cm by 3.5 cm (rectangular) by 0.854 g/cm^2 thick,
U^{238}, 3.7 cm diam (circular) by 1.52 g/cm^2 thick.

The setup and procedure used for the measurements of delayed gamma rays from $Pu^{239}(\gamma,F)$ and $U^{235}(\gamma,F)$ for times greater than about 150 μsec after fission were almost identical to those described in Ref. 3. Except for the use of the liquid scintillator instead of the plastic scintillator, the complete detection system was identical to that used to obtain integral bias bata in the neutron fission experiment (Sec. IIA). The detector and ten identical samples mounted on a rotating wheel

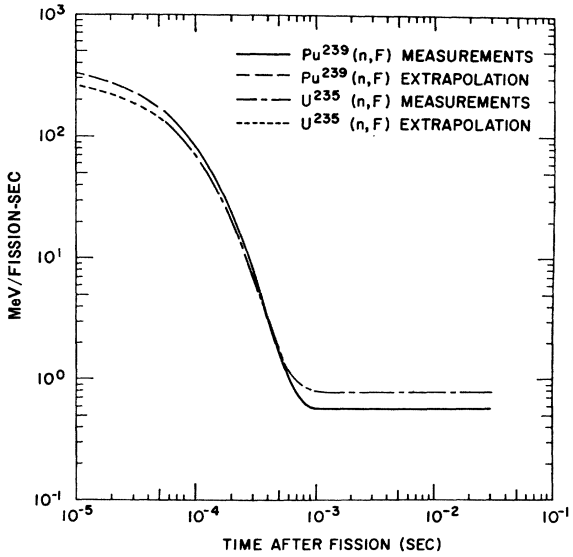

FIG. 10. Absolute gamma-ray energy emission rates (MeV/fission sec) for gamma rays with $E_\gamma > 140$ keV as a function of time after $U^{235}(n,F)$ and $Pu^{239}(n,F)$.

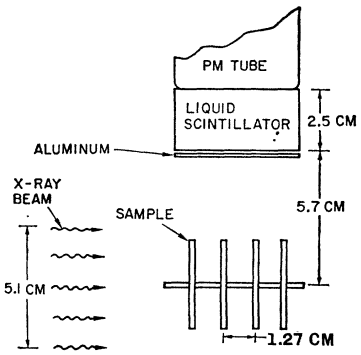

FIG. 11. Detector and sample geometry for photofission measurements.

were enclosed in a shielding cage having large openings for the passage of the x-ray beam. The shielding was effective for times greater than 100 μsec after fission, but was not used for measurements at early times because of the gamma-ray background generated by scattering and absorption of neutrons by the enclosure.

Backgrounds in the photofission measurements consisted of the natural activity of the samples, the activity induced in each sample by preceding pulses, ambient background, and the background from neutrons. Except for the last of these, the backgrounds could be determined in a straightforward manner.[3] Neutrons produced by (γ,F) and (γ,n) reactions in the fissionable samples caused a gamma-ray background that was comparable to the delayed gamma-ray signal and persisted until 15 msec after the beam pulse. This background was determined from measurements with a tungsten background subtraction sample, which served as a neutron source by means of (γ,n) reactions. Three background subtraction samples were used, one for each type of fission sample. Each sample was composed of four units with the same lateral dimensions and space between units as those of the corresponding fission sample. The thickness of the tungsten was adjusted to give the same neutron yield as the fission sample. Relative neutron yields from the tungsten and fissionable samples were determined from measurements with a BF_3 neutron detector embedded in a cadmium-covered block of paraffin.

To obtain data for times less than about 50 μsec, the paralyzing effects on the detector and electronics caused by primary and secondary x rays scattered by the sample during the beam pulse had to be reduced. This was accomplished by decreasing the beam pulse width from 4.5 to 0.2 μsec and, by means of a beam hardener, eliminating the low-energy bremsstrahlung x rays, which are ineffective in producing fissions. The beam hardener, 1.72 m of carbon, was placed in the beam collimator. The reduction in the number of fissions per beam pulse resulting from these changes was partially compensated by using only one sample and increasing the beam repetition rate from 1 to 15 pulse/sec. Because of the high intensity of delayed gamma rays at early times, it was possible to use this repetition rate without generating an excessive long-term activity in the sample.

Amplifier recovery problems in the early-time measurements were avoided by using a 14-stage Phillips 56 AVP photomultiplier tube with no further amplification. During the x-ray beam pulse, the photomultiplier was gated off by placing a bias pulse of 200 V on the focus grid. The fast signal at the anode, which was developed across a 90-Ω resistor, was fed to a tunnel diode discriminator which gave a shaped output signal, 10 Volts high and 0.1 μsec wide. These output pulses were passed through a cable directly to the TMC time analyzer. To set the bias of the tunnel-diode discriminator, the output from the discriminator was used to gate a pulse-height analyzer into which were fed linear signals from the last dynode of the photomultiplier tube. Standard gamma-ray sources were used for the calibration.

To determine if the gain of the photomultiplier changed after the off-gating pulse was removed, the number of counts above a 510-keV bias produced by Cs^{137} gamma rays (662 keV) was measured as a function of time before and after the gating pulse. From these and a pulse-height distribution of the gamma rays, the gain shift was found to vary monotonically with time after the end of the gating pulse from -12.5% at 2 μsec to 0% at 20 μsec. The same measurement was repeated under beam conditions with the tungsten background sample for U^{235} in place and a strong Cs^{137} source near the detector. With the beam pulse occurring 1 μsec before the end of the gating pulse, the gain shift varied from -19.5% at 2 μsec after the gating pulse to 0% at 35 μsec. Since the magnitude of the gain shift was increased by the beam flash, the beam pulse width and amplitude were carefully maintained throughout the early time measurements at the levels used for this test.

As a further check on the performance of this detection system under beam conditions, the decay rate of gamma rays from isomeric transitions produced by $W^{182}(\gamma,n)W^{181m}$ reactions was measured. From previously reported work[8] this isomer is known to decay with a half-life of 14.7±0.5 μsec, emitting a single 368-keV gamma ray. Measurements of the gamma-ray intensitity from the tungsten background sample for U^{235} were performed as a function of time with the integral bias set at 250 keV. The neutron-induced background was determined by normalizing data taken with a bias of 510 keV to the 250-keV data at ~140 μsec, a time at which the activity from the 14.7-μsec isomer had decayed to a negligible level. It was assumed that the time dependence of this background was the same for both biases. The circular data points in Fig. 12 show the decay rate for the tungsten isomer after backgrounds were subtracted, but before corrections were

[8] R. B. Duffield and S. H. Vegors, Jr., Phys. Rev. 112, 1958 (1958).

made for the gain shift. To correct the tungsten decay data, the gain shift measured under beam conditions, together with the response function of the detector for 368-keV gamma rays, was used. The corrected data, also shown in Fig. 12, gave a half-life of 14.0±0.7 μsec, in good agreement with the published value. Hence it was concluded that the data gathered with the detection system were reliable, providing corrections were made for the measured gain shifts.

B. (γ,F) Data

Data on the relative intensity of gamma rays versus time for times greater than about 150 μsec after the photofission of Pu^{239} and U^{235}, as observed with a detector bias set at 510 keV, are shown in Fig. 13. Even

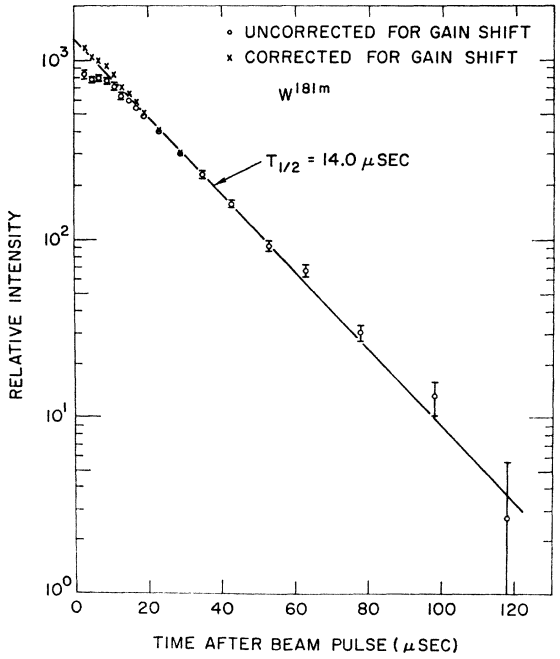

FIG. 12. Intensity of 368-keV gamma rays from the decay of W^{181m} as a function of time after $W^{182}(\gamma,n)$. Data before and after corrections for the photomultiplier gain shift are shown.

though this measurement for U^{235} had been done previously,[3] it was repeated here to provide a direct comparison with the Pu data during the present experiment. The data shown in the figure have been corrected for backgrounds but not for the gamma-ray attenuation and detector efficiency. The error bars indicate the statistical uncertainties only.

Relative intensities of delayed gamma rays measured for U^{235}, U^{238}, and Pu^{239} at early times after fission with a 510-keV bias are shown in Fig. 14. These data have been corrected for backgrounds but not for attenuation, detector efficiency, and detector gain shift. The backgrounds, as evaluated with the appropriate background samples, ranged from about 10% of the net delayed

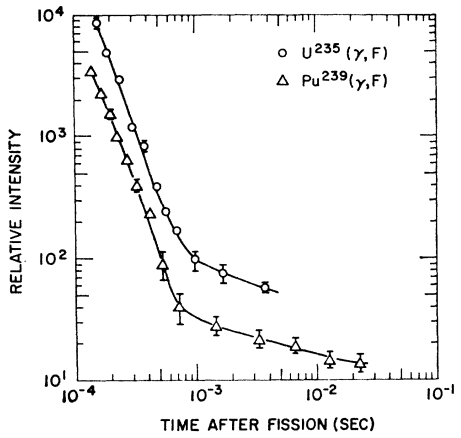

FIG. 13. Relative intensities of gamma rays versus time after the photofission of U^{235} and Pu^{239} for a discriminator bias setting of 510 keV. The Pu data were normalized arbitrarily relative to the U^{235} data. These intensities were corrected for backgrounds but not for detector efficiency and gamma-ray attenuation.

gamma-ray signal at 2 μsec to about 50% of the net signal at 200 μsec. The most striking feature of these new data at early times is the short-lived component with an apparent half-life of a few μsec. The existence of this component for all three target nuclei indicates that it results from fission-fragment isomers.

The integral-bias data on delayed gamma rays from photofission were corrected for the gamma-ray energy dependence of the detector efficiency and the attenuation by the samples using the procedure described earlier (Sec. IIC). For times greater than 20 μsec the

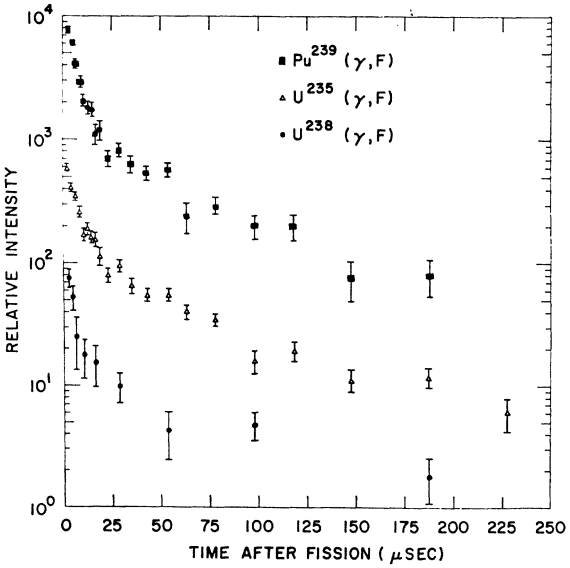

FIG. 14. Relative intensities of gamma rays versus time after the photofission of U^{235}, U^{238}, and Pu^{239} for a discriminator bias setting of 510 keV. Data have been corrected for backgrounds but not for attenuation, detector efficiency, and detector gain shift. The relative intensity for each case of fission has been normalized arbitrarily with respect to the other cases of fission.

gamma-ray energy spectra for neutron fission from the present work (Table I) and the work by Fisher and Engle[5] were used. Although the energy spectrum of delayed gamma rays from photofission may not be identical to that for neutron fission, the error introduced by this assumption is probably small for the following reasons: (1) the correction factor I_p/I_I is relatively insensitive to changes of the relative intensities of the isomeric gamma rays listed in Table I, and (2) since the relative energy spectra of delayed gamma rays at 0.35 sec for the neutron fission of several different nuclei are almost identical,[5] one would expect the energy spectra of photofission gamma rays in the plateau region to have the same shape.

The intensity data at very early times, given in Fig. 14, had to be corrected for the gain shift of the detector as well as for the attenuation and detector efficiency. Since no information was available on the energy spectrum of gamma rays constituting the very short-lived component of decay (~4 μsec apparent half-life), this portion of the decay was separated and corrected using an assumed spectrum. The separation of the observed intensity into a short-lived component "A" and a longer lived component "B" is shown in Fig. 15. Each of the components was corrected separately, and then the two were recombined to form the final corrected intensity. The gamma-ray energy spectrum of component "A" for all the 510-keV data was assumed to be a single gamma-ray line at 900 keV, which is approximately the average energy of the isomeric gamma rays from neutron fission with energies greater than 510 keV (see Table I). To estimate the error which would result from these corrections if the spectrum differed from that assumed, the corrections

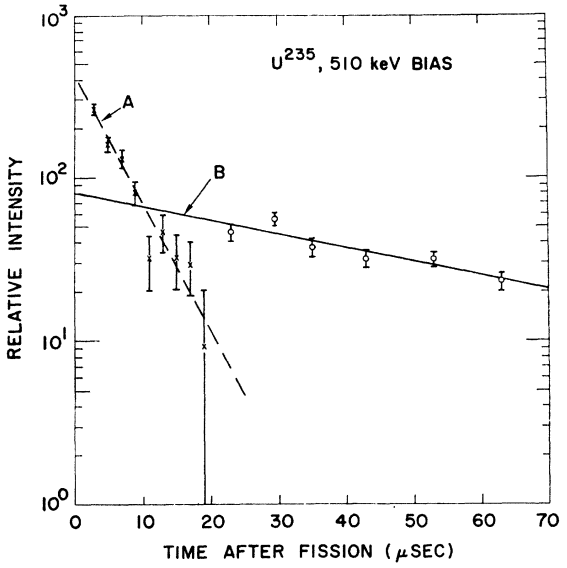

FIG. 15. Intensity versus time of the short-lived component "A" and the longer-lived component "B" of the 510-keV $U^{235}(\gamma,F)$ data.

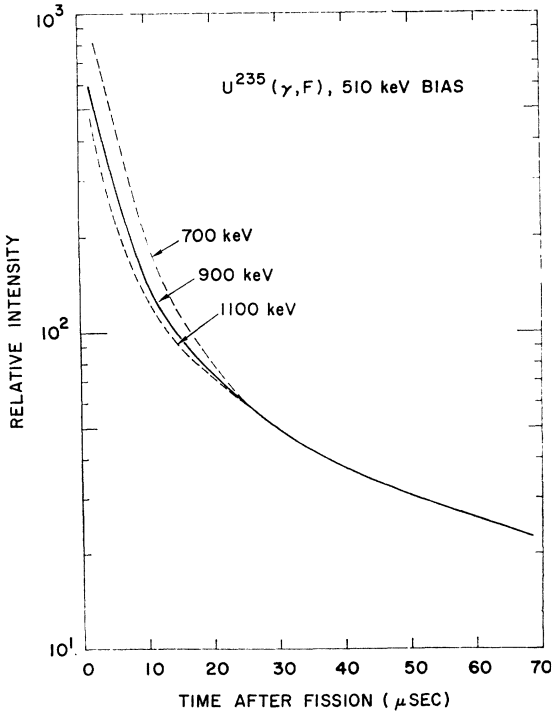

FIG. 16. 510-keV intensity data for $U^{235}(\gamma,F)$ after corrections using a single-energy spectrum of 900 keV for the component "A" of the decay curve. Data resulting from corrections using single energies of 700 and 1100 keV are also given to show the sensitivity to the assumed energy spectrum.

for the U^{235} 510-keV data were also calculated assuming single-energy spectra of 700 and 1100 keV. Correction factors for component "B" were computed using the spectrum of the longer-lived isomers obtained for neutron fission, as discussed above. Smooth curves for the final corrected $U^{235}(\gamma,F)$ data are shown in Fig. 16.

C. Photofission Results

Figure 17 shows smoothed curves of the intensity of gamma rays following the photofission of U^{235}, U^{238}, and Pu^{239} from 2 μsec to the plateau region. The absolute data which were determined previously[3] for U^{235} in the plateau region and for U^{238} for times greater than about 100 μsec are given in these plots. Since an absolute determination of the gamma-ray yield for Pu was not made, the data for this element were normalized in the plateau region using a procedure[3] which is based on Griffin's theory. The corrected data for the earliest time region were normalized to the longer time data between 100 and 200 μsec. The statistical errors for the data points on which the curves are based were generally less than ±15%, except for the U^{238} data at early times ($t<250$ μsec) where the statistical uncertainties were as large as ±25%. The uncertainty in the early-time data resulting from the normalization is approximately ±25% for U^{235} and Pu^{239} and ±30% for U^{238}. An addition error estimated to be ±60% may be present

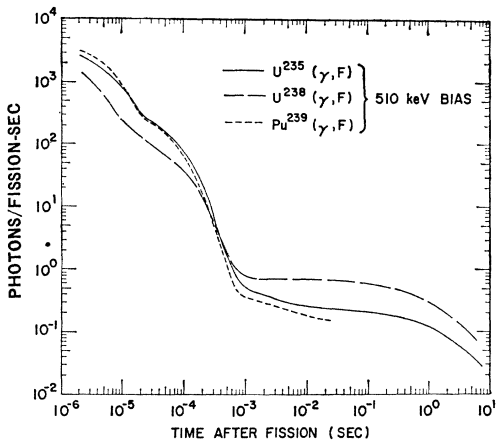

FIG. 17. The absolute intensities of gamma rays (photons/fissions sec) with $E_\gamma > 510$ keV as a function of time after the photofission of U^{235}, U^{238}, and Pu^{239}.

in the data for times less than 20 μsec because of the gamma-ray spectrum assumed for the correction of the data in this time region.

The data given in Fig. 17 show that the intensity of delayed gamma rays with energies greater than 510 keV from $U^{235}(\gamma,F)$ is not greatly different from that for $Pu^{239}(\gamma,F)$ in the time region where the measurements overlap. The U^{235} data are approximately 30% less than the Pu data at 2 μsec and about 50% larger in the plateau region. In contrast the intensity for U^{238} is approximately one-half that for U^{235} or Pu^{239} at the shortest times but is about three times higher in the plateau region. In addition, it is evident from Fig. 17 that the decay curves for $Pu^{239}(\gamma,F)$ and $U^{235}(\gamma,F)$ contain a component with an apparent half-life of a few msec which is not present in the U^{238} data. Because of this msec activity, the normalization of the $Pu(\gamma,F)$ data to the absolute plateau level derived from Griffin's theory[4] was performed in the vicinity of 25 msec.

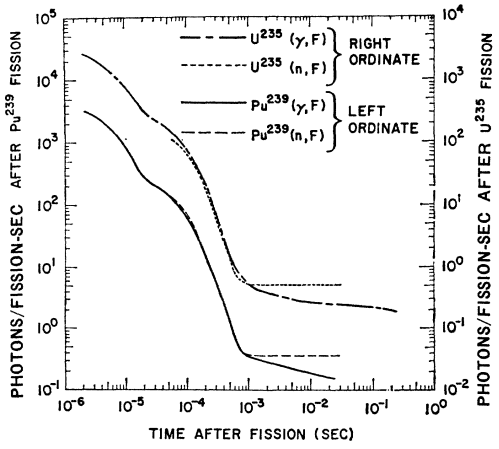

FIG. 18. The absolute intensities of gamma rays with $E_\gamma > 510$ keV as a function of time after the photon- and neutron-induced fission of U^{235} and Pu^{239}.

The absolute intensities of gamma rays with $E_\gamma > 510$ keV versus time after the photon- and neutron-induced fission of U^{235} and Pu^{239} are shown in Fig. 18. For both of these isotopes the intensity of gamma rays in the isomeric region from photofission is approximately the same as that from neutron fission, whereas the intensity in the plateau region is lower for photofission. In addition, the decay component an with apparent half-life of several msec which occurs following the photofission of both U^{235} and Pu^{239} does not occur following neutron fission.

IV. DISCUSSION

The close agreement of the half-lives and relative intensities for the pairs of isomeric gamma rays, (710, 990 keV), (450, 1260 keV), and (250, 850 keV), which were observed in the neutron-fission measurements (see Table I), suggests that there are three isomers, each giving rise to a pair of gamma rays in cascade. This is almost certainly the case provided that the internal conversion coefficients for these transitions are small. Information on the upper limits of the internal conversion coefficients for the transitions can be inferred from the following argument. Each of the proposed cascades probably consists of a slow transition de-exciting the isomeric state followed by a faster transition from the intermediate level to the ground state. Since the emission sequence of the two gamma rays is not known, one must assume that either of the gamma rays can be the one which de-excites the isomeric state. Hence for each gamma ray, the gamma-ray transition probabilities for possible multipole orders were computed using the measured half-life and theoretical values of the internal conversion coefficient[9] for the range of atomic numbers covered by fission fragments. These transition probabilities were then compared with a compilation of experimental results[10] for gamma-ray transitions of known energy and multipolarity to obtain the possible multipole orders which are applicable if the gamma ray in question de-excites an isomeric state. Values of α_{max}, the largest internal conversion coefficient which is consistent with the possible multipolarities, were obtained from tabulations for an atomic number of 59, which is the highest atomic number with a fission yield sufficient to explain the observed gamma ray intensities (see below). The multipole orders and values of α_{max} resulting from the above arguments are presented in Table III. From the results for α_{max} we conclude that the pairs, (450, 1260 keV), (990, 710 keV), and (250, 850 keV) are in cascade. In the

[9] L. A. Sliv and I. M. Band, in *Alpha-, Beta-, and Gamma-Ray Spectroscopy*, edited by K. Siegbahn (North-Holland Publishing Company, Amsterdam, 1965), Vol. 2, Appendix 5.

[10] E. Segrè, *Experimental Nuclear Physics* (John Wiley & Sons, Inc., New York, 1959), Vol. III, Part X.7; J. Lindskog, T. Sundstrom, and P. Sparrman, in *Alpha-, Beta-, and Gamma-Ray Spectroscopy*, edited by K. Siegbahn (North-Holland Publishing Company, Amsterdam, 1965), Vol. 2, Appendix 3.

TABLE III. The possible multipolarities and maximum internal-conversion coefficients for the isomeric transitions which result from the assumption that each of the gamma rays de-excites an isomeric state.

Gamma-ray energy (keV)	Possible multipolarity	α_{max}
250	*E*2, *M*2	0.47
450	*M*2, *E*3	0.077
710	*E*3, *M*3	0.046
850	*E*3, *M*3	0.029
990	*E*3, *M*3	0.016
1260	*E*3, *M*3	0.009

case of the last pair, either gamma ray could de-excite the isomeric state of a nucleus with $Z<49$, since α_{max} for the 250-keV transition is small ($<10\%$) for this range of atomic numbers; however, for $Z>49$, only the de-excitation of the isomeric state by the 850-keV gamma ray would be consistent with the measured intensities of the two gamma rays.

The yield per fission of each isomer responsible for a pair of cascade gamma rays was computed from the average of the half-lives and absolute intensities given in Table I for the two gamma rays. These yields are presented in Table IV. Comparison of these yields with abundances of fission products given in the literature[11] indicate that all three isomers fall within the approximate ranges of atomic number and mass (Z,A) from (33, 84) to (43, 105) and from (50, 129) to (59, 150), i.e., the regions containing the peaks in the mass yield curve. The limits on Z and A were determined assuming the ratio of the isomeric state yield to the sum of the ground state and isomeric state yields to be unity. This assumption seems reasonable since previous measurements of this ratio gave results between 0.61 and 0.77 for two longer lived isomers formed in four different cases of thermal-neutron fission.[12]

[11] R. C. Bolles and N. E. Ballou, U. S. Naval Radiological Defense Laboratory, San Francisco, Report 456, 1956 (unpublished); L. R. Bunney, E. M. Scadder, J. O. Abriam, and N. E. Ballou, in *Second United Nations Conference on the Peaceful Uses of Atomic Energy, Geneva, 1958* (United Nations, Geneva, 1958), Vol. 15, p. 444; M. P. Anikina, P. M. Aron, V. K. Gorshkov, R. N. Ivanov, L. M. Krizhansky, G. M. Kukaradze, A. N. Murin, I. A. Reformatsky, and B. V. Ershler, *ibid.*, p. 446.

TABLE IV. Summary of half-lives, energies of cascade gamma rays, and yield per fission of isomers observed after $Pu^{239}(n,F)$ and $U^{235}(n,F)$.

Isomer half-life (μsec)	Energies of cascade gamma rays	Fission yield in percent $Pu^{239}(n,F)$	Fission yield in percent $U^{235}(n,F)$
80	1260, 450 keV	0.46	0.32
54	850, 250 keV	0.76	0.89
32	990, 710 keV	0.57	0.35

The present photofission data show that additional isomers with half-lives of the order of a few μsec are also produced in fission. The results of the photon- and neutron-induced fission measurements are consistent with expectations that a number of isomers should exist following fission, since the fission fragments are believed to emerge with high intrinsic angular momenta which are not greatly changed by prompt-neutron emission.[2,12]

ACKNOWLEDGMENTS

We are grateful to Dr. J. R. Beyster for helpful discussions throughout the course of the work, to the LINAC operators for their help with the beam, and to A. Dolinski and P. Phelps for assembling the experimental gear. Valuable discussions were held with Dr. J. Malik, Dr. Paul Caldwell, and Major W. Henderson.

[12] D. G. Sarantites, G. E. Gordon, and C. D. Coryell, Phys. Rev. **138**, B353 (1965).

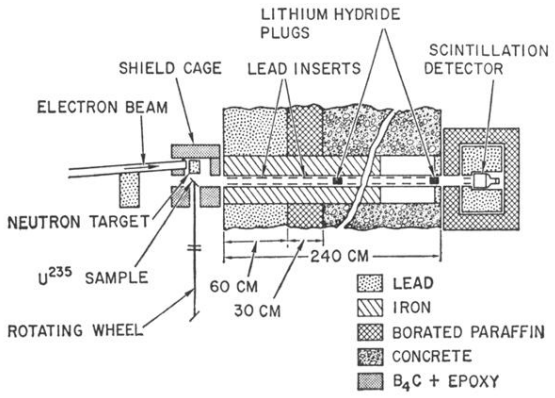

FIG. 1. Schematic drawing of the configuration used for studies of delayed gamma rays from neutron fission.

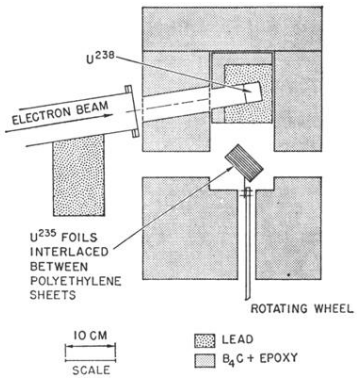

FIG. 2. Details of the sample and source configuration for measurements of delayed gamma rays from neutron fission.